


RESEARCH ARTICLE

Open Access



Bupi Yishen formula attenuates kidney injury in 5/6 nephrectomized rats via the tryptophan-kynurenic acid-aryl hydrocarbon receptor pathway

Yenan Mo^{1†}, Xina Jie^{1†}, Lixin Wang², Chunlan Ji¹, Yueyu Gu², Zhaoyu Lu^{1,2*}  and Xusheng Liu^{2*}

Abstract

Background: Bupi Yishen Formula (BYF), a patent traditional Chinese medicine (TCM) formulation, has been used in the clinical treatment of chronic kidney disease (CKD). However, the mechanism of action of BYF has not been fully elucidated.

Method: To investigate the variation in the metabolic profile in response to BYF treatment in a rat model of 5/6 nephrectomy (Nx), rats in the treatment groups received low- or high-dose BYF. At the end of the study, serum and kidney samples were collected for biochemical, pathological, and western blotting analysis. Metabolic changes in serum were analyzed by liquid chromatography-tandem mass spectrometry.

Results: The results showed that BYF treatment could reduce kidney injury, inhibit inflammation and improve renal function in a dose-dependent manner. In total, 405 and 195 metabolites were identified in negative and positive ion modes, respectively. Metabolic pathway enrichment analysis of differential metabolites based on the Kyoto Encyclopedia of Genes and Genomes database identified 35 metabolic pathways, 3 of which were related to tryptophan metabolism. High-dose BYF reduced the level of kynurenic acid (KA) by more than 50%, while increasing melatonin 25-fold and indole-3-acetic acid twofold. Expression levels of aryl hydrocarbon receptor (AhR), Cyp1A1, and Cyp1B1 were significantly reduced in the kidney tissue of rats with high-dose BYF, compared to 5/6 Nx rats.

Conclusion: BYF has a reno-protective effect against 5/6 Nx-induced CKD, which may be mediated via inhibition of the tryptophan-KA-AhR pathway.

Keywords: Chronic kidney disease, Bupi Yishen formula, Metabolomics, Kynurenic acid, Aryl hydrocarbon receptor pathway

* Correspondence: luzhaoyu111@163.com; liuxu801@126.com

[†]Yenan Mo and Xina Jie contributed equally to this work.

¹The Second Clinical Medical College, Guangzhou University of Chinese Medicine, Guangzhou 520120, China

²Nephrology Department, the Second Affiliated Hospital of Guangzhou University of Chinese Medicine, Guangdong Provincial Hospital of Chinese Medicine, Guangzhou 520120, China



© The Author(s). 2021 **Open Access** This article is licensed under a Creative Commons Attribution 4.0 International License, which permits use, sharing, adaptation, distribution and reproduction in any medium or format, as long as you give appropriate credit to the original author(s) and the source, provide a link to the Creative Commons licence, and indicate if changes were made. The images or other third party material in this article are included in the article's Creative Commons licence, unless indicated otherwise in a credit line to the material. If material is not included in the article's Creative Commons licence and your intended use is not permitted by statutory regulation or exceeds the permitted use, you will need to obtain permission directly from the copyright holder. To view a copy of this licence, visit <http://creativecommons.org/licenses/by/4.0/>. The Creative Commons Public Domain Dedication waiver (<http://creativecommons.org/publicdomain/zero/1.0/>) applies to the data made available in this article, unless otherwise stated in a credit line to the data.

Background

Chronic kidney disease (CKD) is an emerging epidemic. The overall prevalence of which increased by 29.3% worldwide between 1990 and 2017. In total, it affected 697.5 million people in 2017, for a global prevalence of 9.1%, and is associated with high morbidity and mortality [1]. CKD results in changes in kidney structure and function, eventually leading to end-stage renal disease that requires dialysis or kidney transplantation. Thus, there is an urgent need for effective methods to prevent CKD progression.

In recent years, there has been increasing evidence regarding the beneficial effect of traditional Chinese medicine (TCM) on CKD in humans [2–4] and animals [5–7]. Bupi Yishen Formula (BYF) is a patent TCM formulation modified from the historical TCM prescription, Si-jun-zi Decoction. It was developed based on the results of text mining of medical records from Guangdong Provincial Hospital of Chinese Medicine, a tertiary hospital in southern China. BYF contains nine herbal medicines, including *Astragalus mongholicus* (Huangqi), *Codonopsis pilosula* (Dangshen), *Atractylodes macrocephala* (Baizhu), *Poria cocos* (Fuling), *Dioscorea opposita* (Shanyao), *Coici semen* (Yiyiren), *Polygonum multiflorum* (Heshouwu), *Cuscuta Chinensis* (Tusizi), and *Salvia miltiorrhiza* (Danshen). *Astragalus mongholicus* (Huangqi) and *Salvia miltiorrhiza* (Danshen), a commonly used drug pair for clinical treatment of CKD in traditional Chinese medicine with good efficacy, markedly reduced serum creatinine and urea nitrogen, and ameliorated tubular atrophy and interstitial fibrosis in CKD rats [7]. Our previous study observed that the major compound of *Astragalus membranaceus* (Huangqi), Astragaloside IV, prevented indoxyl sulfate-induced tubulointerstitial injury in mice via attenuation of oxidative stress [8]. *Codonopsis pilosula* (Dangshen) showed its renoprotective effect against renal ischemia/reperfusion in rats by inhibiting the proinflammatory cytokine TNF- α release [9]. *Atractylodes macrocephala* (Baizhu) could increase the level of superoxide dismutase (SOD), decrease the productions of IL-6 and TNF- α , and improve the renal tissue injury on nephrotic syndrome in rats [10]. *Poria cocos* (Fuling) ameliorated cisplatin-induced kidney tubular epithelial cells injury by inhibiting JNK, ERK, p38, and caspase-3 [11]. *Dioscoreaop posita* (Shanyao) could attenuate oxidative stress and fibrosis, regulate lipid metabolism, and inhibit inflammation against renal damage [12, 13]. The natural compound of *Polygonum multiflorum* (Heshouwu) played a protective role in ameliorating the progression of focal segmental glomerulosclerosis in a mouse model via activation of the Nrf2-Keap1 antioxidant pathway [14]. In our previous work, chemical constituents of BYF were systematically investigated by ultra-high-performance liquid chromatography

(UHPLC) with linear ion trap-orbitrap mass spectrometry (MS) and UHPLC with triple-quadrupole tandem MS methods, which provided comprehensive qualitative and quantitative information for analysis of the main components of BYF. Eighty-six compounds, including flavones, phenolic acids, saponins, and other compounds, were identified [15]. Though we have not yet tested the effect of BYF in animals or cells, the major components of BYF have been shown reno-protective effect. Moreover, we have performed a multi-center, double-blind, randomized controlled trial to assess the efficacy and safety of BYF for delaying progression in patients with non-diabetes stage 4 CKD (**HERBAAL trial**) [16]. The result demonstrated that the BYF group experienced slower renal function decline compared to the losartan group over 48 weeks, without significant group differences in the incidence rates of adverse events [17]. However, the underlying mechanism of the effect of BYF on CKD is unclear.

Metabolomics is an evolving research area, with numerous successes in terms of characterizing biochemical metabolites related to disease progression, as well as responses to therapeutic interventions [18]. Therefore, metabolomics has been widely used to evaluate the efficacy and potential mechanisms of action of TCM prescriptions and herbs [7, 19, 20], thus facilitating the modernization of TCM. 5/6 nephrectomy (Nx) is the most classic CKD model as the glomerulosclerosis and tubulointerstitial fibrosis that develop after the 5/6 nephrectomy have been generally considered to represent the adverse consequences of a severe reduction in the number of nephrons [21].

In this study, we aimed to explore the beneficial effects of BYF on CKD, as well as its potential mechanisms of action, in 5/6 nephrectomized (Nx) rats. The characteristics of CKD and effects of BYF treatment were evaluated according to blood biochemical indexes and renal pathological changes. An untargeted metabolomics method, liquid chromatography-mass spectrometry/mass spectrometry (LC-MS/MS), was used for metabolic profiling, to investigate the response to BYF treatment of 5/6Nx CKD rats. Signaling pathways were examined by western blotting. Our findings validate the efficacy and mechanism of BYF, which may offer a promising approach for treatment of CKD in clinical practice.

Methods

Extract preparation and chemical analysis of BYF extract

The medicinal materials used to produce BYF were purchased from Kangmei Pharmaceutical Co., Ltd. (Guangdong, China). Information regarding components of BYF (e.g., Chinese, Latin and English names, medical parts, and places of origin) is shown in Suppl. Table 1. The nine herbs were mixed at the prescribed ratios, extracted

three times (60 min) with boiling water (1:8), and filtered with gauze. The filtered BYF extract was obtained by solvent evaporation in a vacuum at 56 °C.

High-performance liquid chromatography (HPLC) was performed to verify the similarity of the major compounds in BYF prepared in this study and our previous study, in which the chemical constituents of BYF were systematically investigated by HPLC. The HPLC method is described in Suppl. Item 1.

Experimental animals and medicinal intervention

Male Sprague–Dawley rats (specific pathogen-free grade; weight, 180–220 g) were purchased from the Laboratory Animal Center of Southern Medical University (Guangzhou, China). The rats were housed in a specific pathogen-free animal breeding room in Guangdong Provincial Hospital and given free access to water. The rats were fed according to a 12-h light/dark cycle. All experiments were evaluated and approved by the Ethics Committee of Animal Experiments, Guangdong Provincial Hospital of Chinese Medicine (approval no. 2019026).

Forty-six rats were randomly divided into the sham group ($n = 10$) and the CKD group ($n = 36$). CKD was induced by 5/6Nx in rats as follows. All rats were anesthetized with an intraperitoneal injection of 2.0% pentobarbital sodium (30 mg/kg body weight). Two-thirds of the left kidney was initially removed. Seven days later, total right Nx was performed. Rats in the sham group only underwent removal of the fat sac, without Nx (Fig. 1A).

Four weeks after surgery, the CKD group was randomly divided into the 5/6Nx, L-BYF, and H-BYF groups, according to the random number table method. BYF-treated rats received low-dose BYF (3.2 g/kg.w) or high-dose BYF (6.4 g/kg.w) by intragastric administration, once daily. Based on the clinical usage [17] and the Meeh-Rubner equation [22] of dose conversion, 3.2 g/kg and 6.4 g/kg dosage was chosen for low-dose BYF and high-dose BYF, respectively.

Rats in the sham and 5/6Nx groups received an identical volume of normal saline. Body weight was recorded once weekly throughout the experiment. BYF intervention lasted for four weeks. At the end point of the experiment, rats were anesthetized with an intraperitoneal injection of 2.0% pentobarbital sodium (30 mg/kg body weight). When rats became unconscious, they were euthanized using cervical dislocation. Blood and kidney tissues were collected and processed for untargeted metabolomic, histological, and western blotting analyses.

Biochemical analysis and enzyme-linked immunosorbent assay

Serum creatinine and blood urea nitrogen were measured by Cobas C702 automatic analyzers (Roche, Basel,

Switzerland). Proteinuria was measured using a bicinchoninic acid protein detection kit (Thermo Fisher Scientific, Waltham, MA, USA). Serum levels of interleukin (IL)-6 and IL-1 β were measured in accordance with the enzyme-linked immunosorbent assay kit instructions (R&D Systems, Minneapolis, MN, USA).

Histological analysis

The kidney tissues of rats were fixed with paraformaldehyde, and then dehydrated and embedded in paraffin. Paraffin-embedded tissues were cut into 3- μ m sections and stained with hematoxylin and eosin (Boster Bio, Wuhan, China).

Immunohistochemistry

Paraffin-embedded rat kidney slides were deparaffined, rehydrated, and immersed in 3% hydrogen peroxide for 10 min at room temperature to block endogenous peroxidase activity. All sections were heated in Tris-EDTA buffer (pH 9.0, Boster, Wuhan, China), blocked with 5% blocking buffer for 30 min at 37 °C, incubated with primary antibodies against Tumor necrosis factor (TNF- α) (1:100, Abcam Cat# ab6671, Cambridge, England), IL-6 (1:100, Abcam Cat# ab9324, Cambridge, England) at 4 °C overnight, incubated with species-specific secondary antibody (SV0004, Boster, Wuhan, China), developed with 3,3'-diaminobenzidine (DAB, Invitrogen, California, USA) and counterstained with hematoxylin. The integrated optical density (IOD) values of the positive staining areas were measured by ImagePro Plus 6.0 software (Media Cybernetics, CA, USA).

Sample preparation and LC-MS/MS analysis for metabolomics

Sample preparation: 100- μ L samples were extracted by direct addition of 300 μ L of precooled methanol and acetonitrile (2:1, v/v). Internal standard mixes 1 and 2 were added for sample preparation quality control (QC). After samples had been vortexed for 1 min and incubated at -20 °C for 2 h, they were centrifuged at 4000 rpm for 20 min. The supernatants were subjected to vacuum freeze-drying. The dried metabolites were resuspended in 150 μ L of 50% methanol for 30 min and centrifuged at 4000 rpm. The supernatants were then transferred to sample vials for LC-MS/MS analysis. A QC sample was prepared by blending the same volume of each sample to evaluate the reproducibility of the overall LC-MS/MS analysis, as described in Suppl. Item 2.

Global metabolomics analysis by LC-MS/MS: Samples were analyzed on a Waters 2D UHPLC column (Waters, Milford, MA, USA), coupled to a Q-Exactive mass spectrometer (Thermo Fisher Scientific) using a heated electrospray ionization source, controlled by Xcalibur 2.3

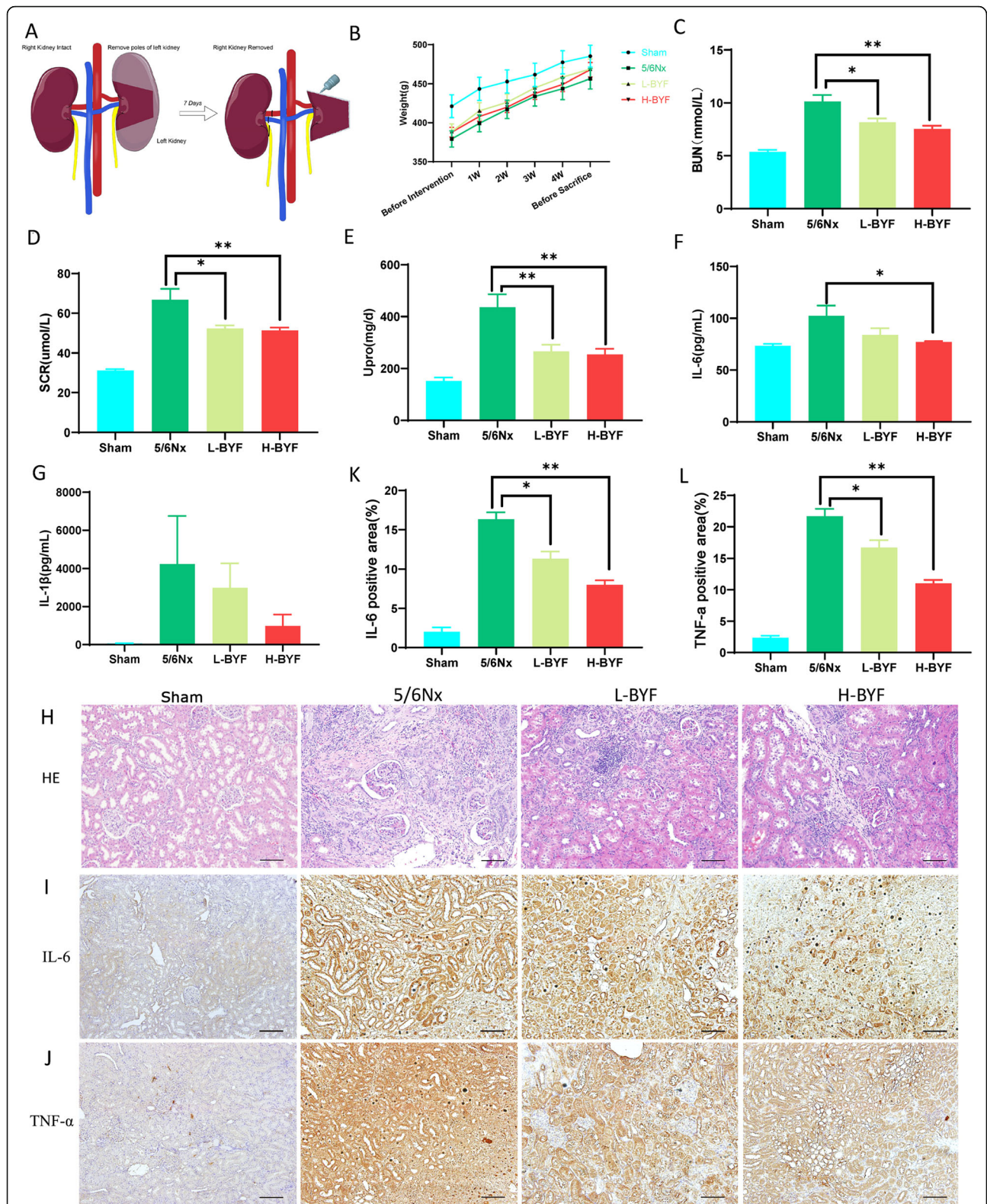


Fig. 1 Effects of BYF on 5/6Nx CKD rats. **(A)** 5/6Nx method. **(B)** Body weight. **(C)** Blood urea nitrogen. **(D)** Serum creatinine. **(E)** Twenty-four-hour urinary protein quantitation. **(F)** Serum IL-6. **(G)** Serum IL-1β. **(H)** Hematoxylin and eosin staining of kidney tissues. **(I-K)** Immunohistochemical staining of TNF-α and IL-6 expression in kidney. Data are presented as the means ± standard error of the mean. *n* = 12 rats per group in the 5/6Nx, L-BYF, and H-BYF groups; *n* = 10 in the sham group (**P* < 0.05, ***P* < 0.001)

software (Thermo Fisher Scientific). Chromatographic separation was carried out on a Waters ACQUITY UHPLC BEH C18 column (1.7 μm , 2.1 mm \times 100 mm; Waters), with the column temperature maintained at 45 °C. The normal mobile phase was 0.1% formic acid (A) and acetonitrile (B) in positive ion mode. In negative ion mode, the mobile phase was 10 mM ammonium formate (A) and acetonitrile (B). The gradient conditions were as follows: 0–1 min, 2% B; 1–9 min, 2% B to 98% B; 9–12 min, 98% B; 12–12.1 min, 98% B to 2% B; and 12.1–15 min, 2% B. The flow rate was 0.35 mL/min, and the injection volume was 5 μL .

The mass spectra of the positive/negative ion modes were captured using the following settings: spray voltage, 3.8/–3.2 kV; gas flow rate in sheath, 40 arbitrary units; aux gas flow rate, 10 arbitrary units; aux gas heater temperature, 350 °C; and capillary temperature, 320 °C. The full scanning range was 70–1050 m/z with a resolution of 70,000, and the automatic gain control target for MS acquisitions was set to 3e6 with a maximum ion injection time of 100 ms. The top three precursors were selected for subsequent MS/MS fragmentation with a maximum ion injection time of 50 ms and resolution of 17,500, using an automatic gain control of 1e5. The stepped normalized collision energies were set to 20, 40, and 60 eV. Nitrogen was used as atomizer and auxiliary gas. The serum samples were analyzed in positive and negative ion modes, and the scanning mass-to-charge (m/z) range was 50 to 1500 Da.

To analyze metabolomic data, the mass spectrum data were processed for noise reduction, peak alignment, and peak identification. Peak intensities were normalized using internal standards. Differential metabolites were analyzed using partial least square-discriminant analysis. Differential metabolites among groups were characterized by a variable importance value > 1 , fold-change ≥ 1.2 or ≤ 0.83 , and q -value < 0.05 . By comparison with databases including ChemSpider (www.chemspider.com) and HMDB (www.hmdb.ca), differential metabolites were preliminarily identified based on the mass fragmentation patterns. Pathway analysis was performed using the Kyoto Encyclopedia of Genes and Genomes (KEGG) database.

Western blotting analysis

Kidney tissues were lysed in 1 mL radioimmunoprecipitation assay lysis buffer containing 1 mM phenylmethyl sulfonyl fluoride and 1% phosphatase inhibitor cocktail (Thermo Fisher Scientific). A bicinchoninic acid protein detection kit was used to detect protein concentrations. Protein samples (50 μg) were boiled with sodium dodecyl sulfate polyacrylamide gel electrophoresis loading buffer, then electrophoresed on a 10% polyacrylamide gel under denaturing conditions and wet-transferred to

polyvinylidene difluoride membranes (Millipore, Burlington, MA, USA). Membranes were exposed to blocking buffer for 2 h and hybridized with primary antibody against aryl hydrocarbon receptor (AhR) (1:500; Abcam, Cat# ab84833 Cambridge, UK), CYP1A1 (1:400; Santa Cruz Biotechnology, Cat# sc-25304, CA, USA), CyP1B1 (1:6000; Abcam, Cat# ab185954, Cambridge, UK), or β -actin (1:2000; Cell Signaling Technologies, Cat# 4970S, Boston, USA) overnight at 4 °C, followed by horseradish peroxidase-labeled anti-rabbit IgG (1:3000, Cell Signaling Technologies, Cat# 7074S, Boston, USA) or anti-mouse IgG (1:3000, Cell Signaling Technologies, Cat# 7076S, Boston, USA) at room temperature. Membranes were washed and then visualized using an enhanced chemiluminescence detection system (Bio-Rad, Hercules, CA, USA). The signals were captured and analyzed using Image Lab System (Bio-Rad).

Statistical analysis

SPSS software (version 18.0, SPSS, Inc., Chicago, IL, USA) was used for statistical analysis. All data with normal distributions are presented as the mean \pm standard error of the mean. Differences between groups were determined by one-way analysis of variance, followed by the Tukey test. Differences were considered statistically significant at $p < 0.05$.

Results

QC of BYF

HPLC indicated that the major components in BYF were similar between this study and the previous study, as shown in Suppl. Fig. 1.

BYF alleviated renal failure phenotypes in CKD rats

We first evaluated the protective effect of BYF on CKD. It is common for patients with CKD to experience weight loss. Notably, L-BYF and H-BYF appeared to promote weight gain in CKD rats compared to 5/6Nx rats, although weight did not significantly differ among groups (Fig. 1B). Blood urea nitrogen, serum creatinine, and 24-h proteinuria levels were significantly higher in the 5/6Nx group than in the sham group. These levels decreased in the BYF-treated groups in a dose-dependent manner (Fig. 1C–E). With regard to the systematic inflammatory response, serum IL-6 and serum IL-1 β were elevated in 5/6Nx rats compared to sham rats, and BYF treatment significantly decreased the serum IL-6 and tended to reduce the serum IL-1 β (Fig. 1F, G).

Consistent with the improved renal function and inhibited inflammation, histopathological changes were improved by low- and high-dose BYF treatments. Hematoxylin and eosin staining of renal tissues showed obvious mononuclear lymphocyte infiltration,

enlargement of the renal tubular lumen, interstitial fibrosis, and renal tubular atrophy in the 5/6Nx group (Fig. 1H). Compared to sham rats, the expression of IL-6 and TNF- α in kidneys were elevated in 5/6Nx rats and BYF significantly reduced kidney IL-6 and TNF- α (Fig. 1I-L).

Global metabolic profiling of serum metabolites in CKD rats

Assessment of data quality using LC-MS/MS

Metabolomics assessment of serum samples from each group was performed with LC-MS/MS, in both positive and negative ion modes. The overlapping total ion current chromatograms of QC samples indicated that the variations during large-scale sample analysis were acceptable (Fig. 2A, B). To ensure that the LC-MS system was stable, principle component analysis was performed, which revealed that all QC samples were consistently clustered together (Fig. 2C, D). The ratio between the number of compounds with <30% coefficient of variation of the relative peak area in QC samples and all compounds detected was greater than 60% (Fig. 2E, F). These results indicated that the LC-MS method was repeatable and stable, and thus suitable for further analysis.

Metabolic profiles of 5/6Nx and H-BYF rats

To evaluate the metabolic changes in CKD rats, principle component analysis was used. The initial metabolic state of the 5/6Nx group was markedly different from that of the H-BYF group (Fig. 3A, B), which demonstrated that BYF treatment significantly altered the serum metabolic profile in CKD rats.

To further compare the metabolic changes between the 5/6Nx and H-BYF groups, partial least square-discriminant analysis was performed. Metabolites with a variable importance value > 1, fold-change ≥ 1.2 or ≤ 0.83 , and q-value < 0.05 were defined as differential metabolites among the groups. In total, 405 and 195 metabolites with significant changes in peak intensity were detected in negative ion mode (123 upregulated and 72 downregulated metabolites, respectively) and positive ion mode (293 upregulated and 112 downregulated metabolites, respectively) (Fig. 3C, D).

Metabolic pathway analysis of BYF effects on CKD rats

To explore the functional significance of the serum metabolic changes in the BYF group, metabolic pathway enrichment analysis of differential metabolites was carried out using the KEGG database. There were 35 metabolic pathways (20 and 23 metabolic pathways in negative and positive ion modes, respectively), including neuroactive ligand-receptor interaction, thiamine metabolism, steroid hormone biosynthesis, metabolic pathways, primary bile acid biosynthesis, tyrosine and

tryptophan biosynthesis, tryptophan metabolism, phenylalanine-bile secretion, bile secretion, regulation of actin cytoskeleton, circadian entrainment, parathyroid hormone synthesis, secretion, and action, biosynthesis of amino acids, aldosterone synthesis and secretion, cholinergic synapse, dopaminergic synapse, insulin secretion, synaptic vesicle cycle, gastric acid secretion, pancreatic secretion, oxidative phosphorylation, salivary secretion, retrograde endocannabinoid signaling, glutathione metabolism, thermogenesis, cAMP signaling pathway, protein digestion and absorption, glycine, serine and threonine metabolism, aminoacyl-tRNA biosynthesis, mineral absorption, lysine degradation, phosphonate and phosphinate metabolism, taste transduction, glyoxylate and dicarboxylate metabolism, and inflammatory mediator regulation of tryptophan channels (Fig. 3E, F).

BYF significantly inhibited tryptophan-KA-AhR pathway

Three of the thirty-five metabolic enrichment pathways were related to tryptophan metabolism. Tryptophan metabolism involves three pathways: indole, kynurenine, and serotonin (Fig. 4). The level of tryptophan did not differ among groups. High-dose BYF treatment reduced the level of kynurenic acid (KA) by more than 50%, while increasing the level of melatonin 25-fold and the level of indole-3-acetic acid twofold (Fig. 5A-D). KA is a type of uremic toxin produced from tryptophan and an endogenous ligand of the AhR. To determine whether BYF treatment influenced the AhR pathway in kidney tissues, the expression levels of AhR, Cyp1A1, and Cyp1B1 were measured by western blotting. The results showed that BYF treatment significantly inhibited AhR signaling in a dose-dependent manner (Fig. 5E).

Discussion

BYF treatment markedly improved kidney function, reduced proteinuria, inhibited the inflammatory response, and alleviated interstitial fibrosis and tubular atrophy in CKD rats in a dose-dependent manner. Metabolomics analysis indicated that BYF regulated tryptophan metabolism and reduced KA production. Expression levels of AhR, Cyp1A1, and Cyp1B1 in kidney tissue were significantly reduced in rats that received BYF treatment compared to 5/6Nx rats. Therefore, BYF treatment may protect the kidney through inhibition of the tryptophan-KA-AhR pathway in CKD rats.

Because of the limited usefulness of angiotensin-converting enzyme inhibitors/angiotensin II receptor blockers in patients with advanced CKD, there is an urgent need for additional renal protective therapies. BYF was shown to slow renal function decline, compared to losartan, over 48 weeks in a multi-center, double-blind, randomized controlled trial [17]. In previous studies by our group, compounds contained in BYF were identified

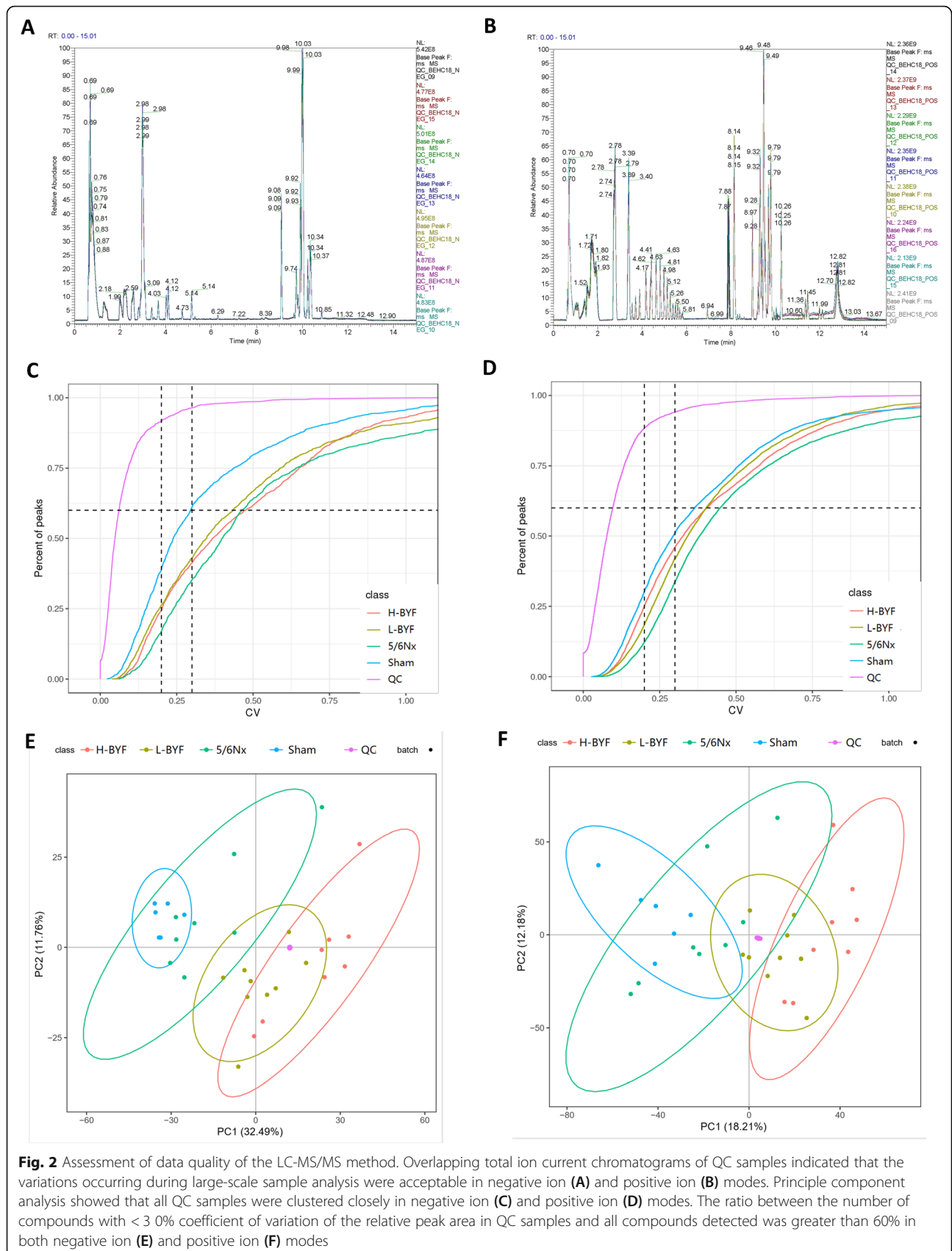


Fig. 2 Assessment of data quality of the LC-MS/MS method. Overlapping total ion current chromatograms of QC samples indicated that the variations occurring during large-scale sample analysis were acceptable in negative ion (A) and positive ion (B) modes. Principle component analysis showed that all QC samples were clustered closely in negative ion (C) and positive ion (D) modes. The ratio between the number of compounds with < 3.0% coefficient of variation of the relative peak area in QC samples and all compounds detected was greater than 60% in both negative ion (E) and positive ion (F) modes

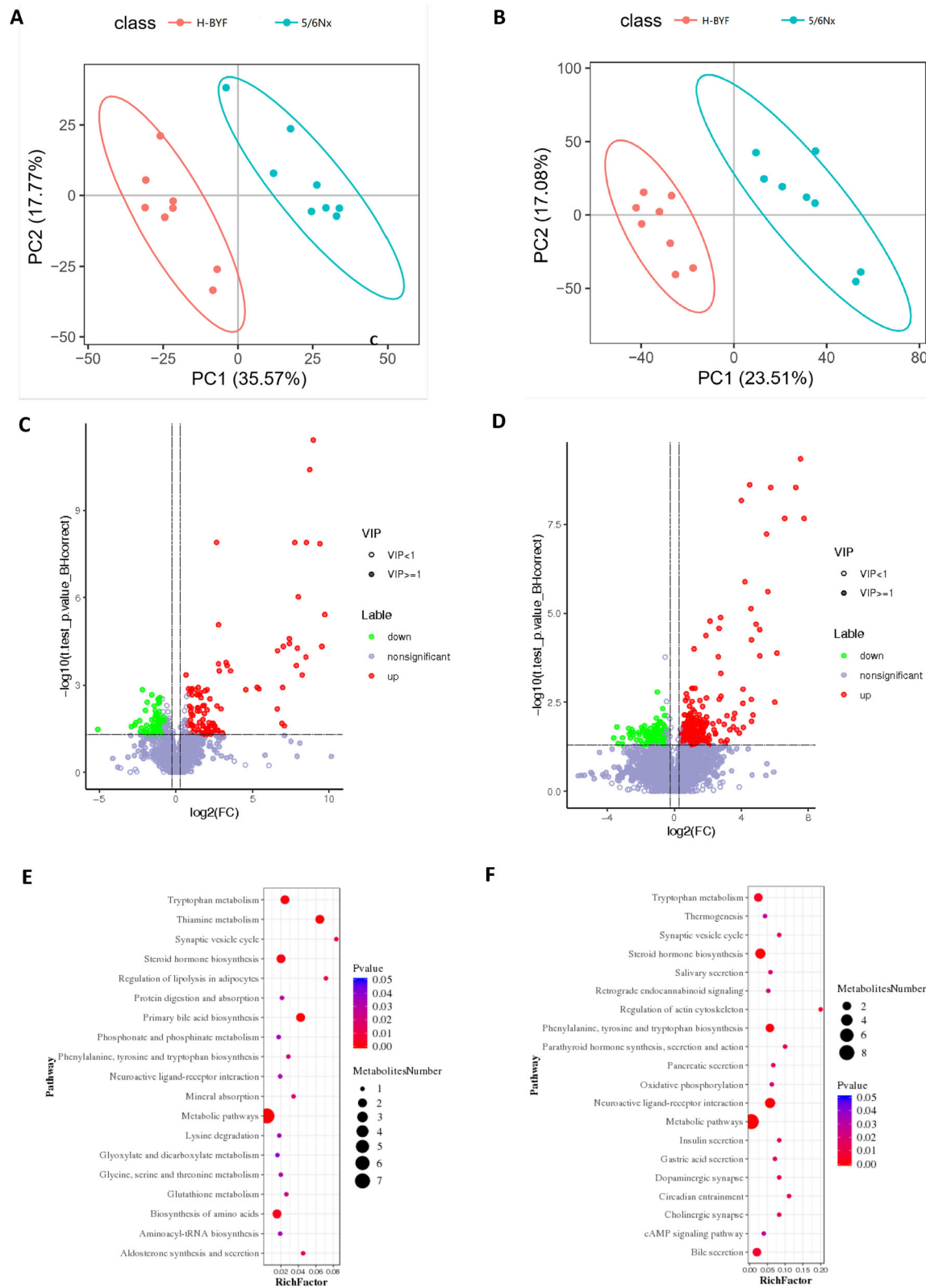


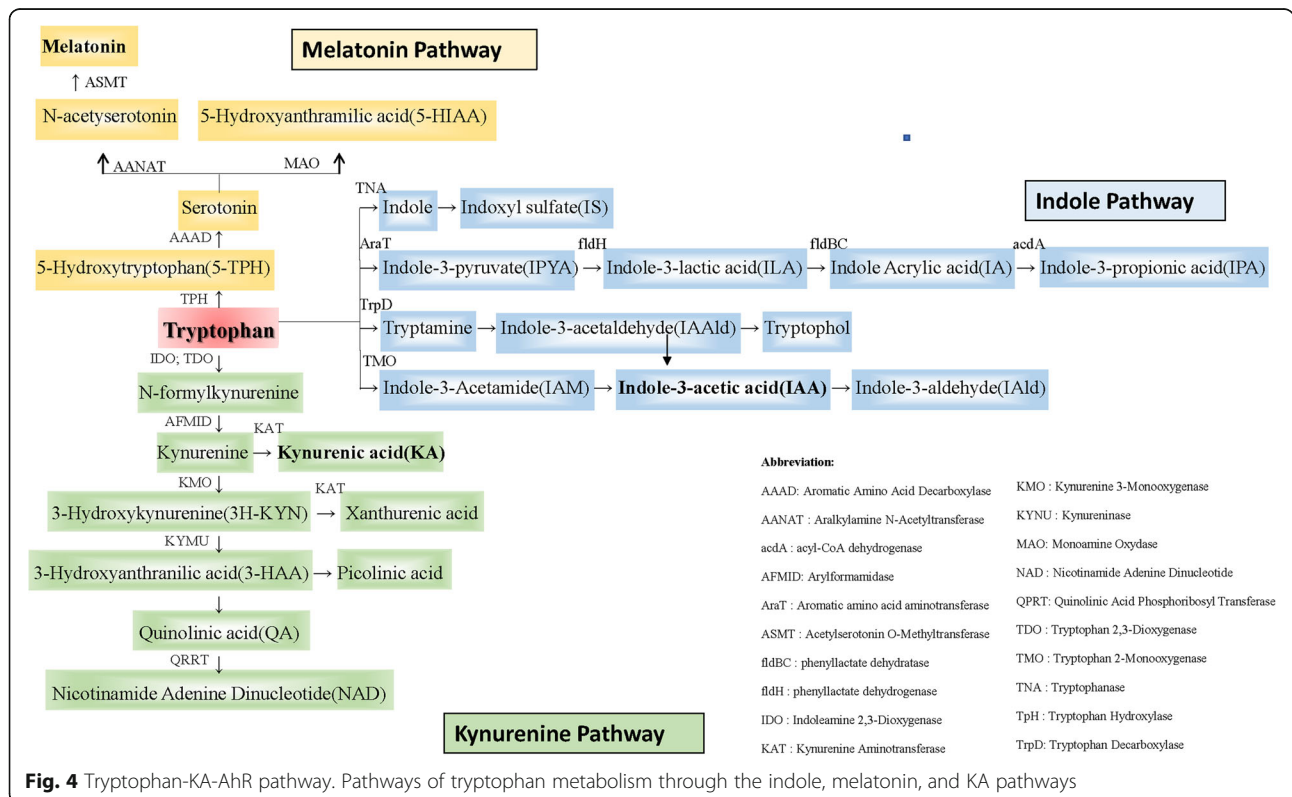
Fig. 3 (See legend on next page.)

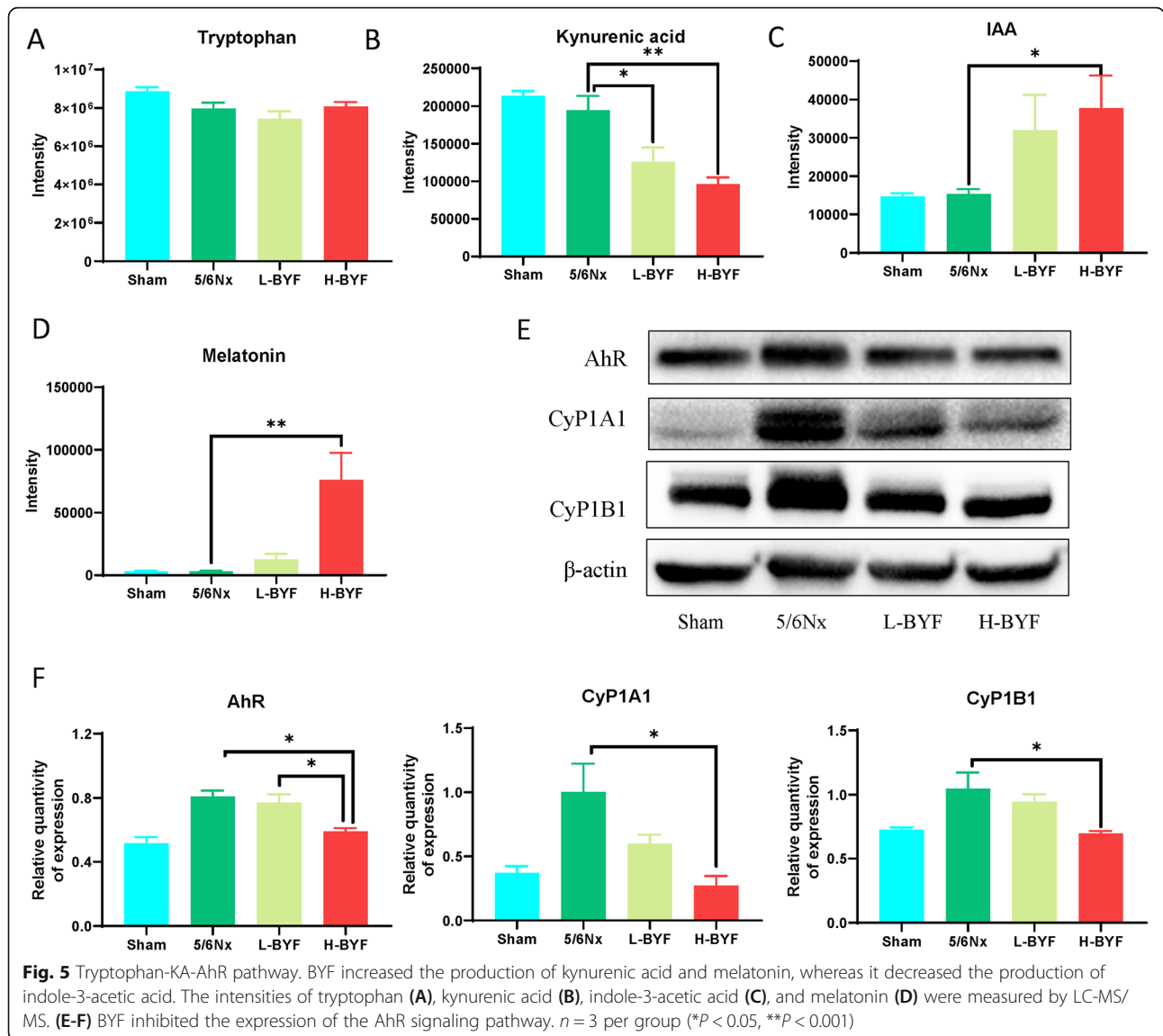
(See figure on previous page.)

Fig. 3 Metabolic profile differences between the 5/6Nx and H-BYF groups. Principle component analysis score plots of serum metabolites: comparison between the 5/6Nx and H-BYF groups in negative ion (A) and positive ion (B) modes. Volcano plot for differential metabolites between the 5/6Nx and H-BYF groups in negative ion (C) and positive ion (D) modes. Bubble plots of KEGG pathway enrichment analysis between 5/6Nx and H-BYF groups in negative ion (E) and positive ion (F) modes

by UHPLC-MS. Specifically, 15 flavones, 10 saponins, 12 phenolic acids, and 49 other compounds were detected [15]. According to TCM theory, Qi deficiency and blood stasis (Qi-Xu-Xue-Yu) occur during the progression of CKD [23]. *Astragalus mongholicus* (Huangqi) are commonly combined to replenish Qi, while *Salvia miltiorrhiza* (Danshen) is often used to activate blood. The effects of Huangqi and/or Danshen on metabolic pathways in rat models of CKD and other diseases have been reported in previous studies [7, 24, 25]. Astragaloside IV is one of the main active ingredients of *Astragalus mongholicus* and is used as a quality control marker of *Astragalus mongholicus* (Huangqi) in the Chinese Pharmacopeia. Pharmacological effects of Astragaloside IV on renoprotection attributable to its anti-inflammatory, antioxidant, anti-apoptotic properties, and the roles in enhancement of immunity, are associated with multiple signaling pathways, including the AMPK signaling pathway, NF-κB signaling pathway, Nrf2 antioxidant signaling pathways and PKC-α-ERK1/2-NF-κB pathway [26]. On the other hand, salvianolic acid A in *Salvia miltiorrhiza* (Danshen) effectively protects the

kidney against oxidative stress in 5/6Nx rats. One of the pivotal mechanisms for the protective effects of salvianolic acid A on kidney injury was mainly related with its antioxidative roles by activating the Akt/GSK-3β/Nrf2 signaling pathway and inhibiting the NF-κB signaling pathway [27]. Cardioprotective effect of rosmarinic acid in *Salvia miltiorrhiza* (Danshen) against myocardial ischaemia/reperfusion injury via suppression of the NF-κB inflammatory signalling pathway and ROS production in mice [28]. *Poria cocos* (Fuling) treatment inhibited the upregulation of IκB/NF-κB pathway and prevented the downregulation of cytoprotective Keap1/Nrf2 pathway [29]. Atractylenolide I in *Atractylodes macrocephala* (Baizhu) ameliorates sepsis syndrome by reduction of pro-inflammatory cytokines and LPS, and provides an improvement in liver and kidney functions [30]. Therefore, the chemical ingredients contained in the drug compound are complex, and its pharmacological effect is the comprehensive or integrated effect of the multiple active ingredients contained in the compound through multiple pathways, multiple links, and multiple targets, and the mechanism of action is complex.





In agreement with the holistic thinking of TCM, metabolomics has shown potential in bioactivity evaluation and action mechanism of TCM as well as pharmaceutical research and development. Compared with transcriptomics, proteomics, and microbiome, metabolomics has the following advantages: firstly, metabolomics amplifies small changes in gene and protein expression, making detection easier. Secondly, metabolomics researchers do not need to establish whole genome sequencing and a large number of expressed sequence tags databases, and the types of metabolites are much smaller than genes, proteins, and microorganisms in quantitative terms. Thirdly, the separation and culture of microorganisms is difficult to achieve the desired effect in microbiome, leading to difficulty in studying bacterial interactions in complex microbial communities, but the technology used in the metabolomics research is more

versatile and easier to be accepted by researchers. Therefore, metabolomics has been applied to discover the mechanism of BYF protecting against CKD.

There was no statistically significant difference between the male and female CKD patients by gender subgroup analysis in our previous clinical RCT. Female rats have menstrual cycles and it is inconvenient to collect 24 h urine, so we chose male rats for this study. In our study, we identified more than 500 significantly different metabolites between H-BYF and 5/6Nx rats with LC-MS/MS-based nontargeted metabolomics. Metabolic pathway enrichment analysis of differential metabolites based on the KEGG database identified 35 metabolic pathways, 3 of which were related to tryptophan metabolism. As an essential aromatic amino acid, tryptophan is a biosynthetic precursor of a variety of host and microbial metabolites [31]. The metabolism of tryptophan

has three major pathways in the gastrointestinal tract (Fig. 4A): 1) the intestinal microorganism-mediated indolic pathway, which transforms tryptophan into several molecules (e.g., indole-3-acetic acid, indole-3-aldehyde, indole-3-propionic acid, and indole-3-acetaldehyde) [32–34]; 2) the kynurenine pathway, which produces kynurenine and downstream products such as KA and quinolinic acid in both immune and epithelial cells via the rate-limiting enzyme, indoleamine 2,3-dioxygenase [35–37]; and 3) the serotonin pathway, which produces melatonin and serotonin in enterochromaffin cells via tryptophan hydroxylase-1 [38]. Indeed, tryptophan-derived uremic toxins, including KA and indole-3-acetic acid, are endogenous agonists of the AhR complex. Tryptophan-derived uremic toxins accumulate in patients with CKD and activate the AhR pathway [39], which results in pro-inflammatory, -oxidant, -apoptotic, and -coagulant effects [40].

Compared to our 5/6Nx rats, H-BYF rats produced more KA but less melatonin and indole-3-acetic acid. These findings indicated that BYF might inhibit the kynurenine pathway, while facilitating a shift toward the serotonin and indole pathways. KA is a stable end product of the kynurenine pathway, whereas kynurenine is not. Thus, KA is the most sensitive marker of kynurenine pathway activation, which is closely associated with the presence and/or development of kidney dysfunction/failure [41]. Lower kidney clearance of KA was associated with significantly greater risk of CKD progression compared to indoxyl sulfate [42]. Higher circulating concentrations of KA are associated with greater oxidative stress and incident myocardial infarction [43, 44]. A large proportion (95%) of tryptophan is metabolized through the kynurenine pathway, which generates considerably more metabolites than the other two pathways. Plasma concentrations of strongly protein-bound toxins are reportedly higher in patients with CKD than in healthy individuals (KA: 75-fold [45, 46], indoxyl sulfate: 72-fold [47, 48], and indole-3-acetic acid: 2.4-fold [48]). In addition, the 1-methyltryptophan led to an increase in the plasma levels of KA in pigs, of approximately 5 μ M, which was sufficient to activate AhR because of the high affinity of KA to AhR, even at low micromolar concentrations [49]. Treatment of murine splenocytes with 5 μ M KA exerted a slight proliferative effect, concurrent with increased secretion of IL-1 β and IL-6. This finding suggested that KA exerts its biological effects via AhR [50]. We noted that IL-1 β and IL-6 levels increased with BYF treatment, but not significantly (presumably due to the small sample size). Notably, H-BYF led to reduction of KA by half, while the level of indole-3-acetic acid increased twofold. This inhibited the AhR signaling pathway, reducing the expression levels of AhR, CyP1A1, and CyP1B1. These changes markedly reduced

proteinuria and the inflammatory response, thus improving kidney function and histopathological changes in CKD rats.

Importantly, the production of melatonin was increased with BYF treatment. There is increasing evidence that altered circadian rhythms and serum melatonin levels are common in patients with CKD, and that the production of melatonin declines during the progression of CKD to end-stage renal disease [51]. Melatonin has shown a reno-protective effect in various renal injury animal models. For instance, melatonin suppressed the renin-angiotensin system in the kidney in 5/6Nx models [52], inhibited fibroblast-myofibroblast trans-differentiation during renal fibrosis in unilateral ureteral obstruction mice [53], and mitigated oxidative stress in diabetic nephropathy rats [54].

It has been reported that activated AhR aggravates renal damage and mediates CKD complications, including cardiovascular disease, anaemia, bone disorders, cognitive dysfunction and malnutrition, and that it influences drug metabolism in individuals with CKD [55]. There are two AhR signalling pathways. One is non-canonical AhR signalling, which controls AhR gene expression through non-xenobiotic-responsive element DNA-response elements. AhR signaling pathway also interacts with additional transcriptional factors such as STAT [56], Nrf2 [57], activator protein-1 [58], and NF- κ B [59], by binding to them and modulating their target genes to enhance inflammatory response. In addition, AhR in the cytoplasm can activate other cytoplasmic proteins, like Smads, β -catenin, MAPK family p38 [60], NADPH oxidase, and extracellular signal-regulated kinase. We have discussed the molecular mechanism of several compounds of BYF protecting against kidney injury, which are related to many signaling pathways including AMPK signaling pathway, NF- κ B signaling pathway, Nrf2 antioxidant signaling pathways. However, how AhR interacts with or influences other transcriptional factors and cytoplasmic protein need further study. Integrating transcriptomics and metabolomics might be helpful to answer this question.

We are in an era where the need for novel approaches for delay CKD progression is on its all-time high. Chinese medicines provide a rich of resources for drug discovery and development. Despite the availability of our clinical RCT and present animal study of BYF treatment, there are still some inherent hurdles hinder their clinical translation, including that the oral bioavailability is weak [61] and the role of key components are difficult to determine. Microbial degradation in the gut is one of the most common and identified reasons for poor pharmacokinetic and oral bioavailability. The intestinal flora is involved in the metabolism of nutrients and food, and plays a core role in the conversion of original herbal

medicine components into functional metabolites. Instead of screening functional ingredients directly from herbal extracts, to study the effect of Chinese medicine and gut microbiota using multi-omics approaches seems critical [62].

Conclusion

In our study, an LC-MS/MS-based nontargeted metabolomics approach was used to investigate the renoprotective effects and mechanism of action of BYF in 5/6Nx CKD rats. Treatment with BYF alleviated kidney injury, improved renal function, and partially reversed metabolic abnormalities. Metabolomics analysis indicated that BYF regulated tryptophan metabolism and reduced KA production, while reducing the expression levels of AhR, CyP1A1, and CyP1B1 in kidney tissue. Therefore, we presume that BYF treatment protected the kidney through inhibition of the tryptophan-KA-AhR pathway in CKD rats.

Abbreviations

AhR: aryl hydrocarbon receptor; BYF: Bupi Yishen Formula; CKD: chronic kidney disease; HPLC: high-performance liquid chromatography; IL: interleukin; KA: kynurenic acid; KEGG: Kyoto Encyclopedia of Genes and Genomes; MS: mass spectrometry; Nx: nephrectomy; QC: quality control; TCM: traditional Chinese medicine; UHPLC: ultra-high-performance liquid chromatography.

Supplementary Information

The online version contains supplementary material available at <https://doi.org/10.1186/s12906-021-03376-1>.

Additional file 1: Suppl. Table 1. Information of components in Bupi Yishen Formula (BYF). **Suppl. Item1.** Method of high-performance liquid chromatography in chemical analysis of BYF Extract. **Suppl. Item2.** Reagents used for Liquid chromatography–tandem mass spectrometry. **Suppl. Fig. 1.** HPLC analysis of Bupi Yishen Formula in present study(A) and previous study(B). The denotation peaks 1–7: (1) Calycosin-7-O-Glc, (2) (E)-THSG, (3) Astragalin, (4) Rosmarinic acid, (5) Salvianolic acid A, (6) Salvianolic acid B, (7) Calycosin.

Additional file 2.

Additional file 3.

Acknowledgments

Thanks for technique support by Shenzhen BGI Tech.

Authors' contributions

Study concept and design: XL and ZL. Animal handling and tissue collection: YM, XJ, CJ, YG and ZL. Molecular biology experiments and data analysis: YM, XJ and ZL. Drafting of the manuscript: YM, XJ, ZL and XL. Critical revision of the manuscript for important intellectual content: LW, ZL and XL. Obtained funding: XL. All authors have read and approved the manuscript.

Funding

This study was supported by the National Natural Science Foundation of China (No. 81873261, Grant Recipient: Xusheng Liu). The funders had no role in study design, data collection and analysis, decision to publish, or preparation of the manuscript.

Availability of data and materials

The datasets used and analyzed during the current study are available from the corresponding author on reasonable request.

Declarations

Ethics approval and consent to participate

All experiments were evaluated and approved by the Ethics Committee of Animal Experiments, Guangdong Provincial Hospital of Chinese Medicine (approval no. 2019026).

Consent for publication

Not applicable.

Competing interests

All authors declare no conflicts of interest.

Received: 7 November 2020 Accepted: 6 July 2021

Published online: 10 August 2021

References

- Bikbov B, Purcell CA, Levey AS, Smith M, Abdoli A, Abebe M, et al. Global, regional, and national burden of chronic kidney disease, 1990–2017: a systematic analysis for the global burden of disease study 2017. *Lancet*. 2020;395(10225):709–33. [https://doi.org/10.1016/S0140-6736\(20\)30045-3](https://doi.org/10.1016/S0140-6736(20)30045-3).
- Lin MY, Chiu YW, Chang JS, Lin HL, Lee CT, Chiu GF, et al. Association of prescribed Chinese herbal medicine use with risk of end-stage renal disease in patients with chronic kidney disease. *Kidney Int*. 2015;88(6):1365–73. <https://doi.org/10.1038/ki.2015.226>.
- Zheng Y, Cai GY, He LQ, Lin HL, Cheng XH, Wang NS, et al. Efficacy and safety of Niaoduqing particles for delaying moderate-to-severe renal dysfunction: a randomized, double-blind, placebo-controlled, multicenter clinical study. *Chin Med J*. 2017;130(20):2402–9. <https://doi.org/10.4103/0366-6999.216407>.
- Wang YJ, He LQ, Sun W, Lu Y, Wang XQ, Zhang PQ, et al. Optimized project of traditional Chinese medicine in treating chronic kidney disease stage 3: a multicenter double-blinded randomized controlled trial. *J Ethnopharmacol*. 2012;139(3):757–64. <https://doi.org/10.1016/j.jep.2011.12.009>.
- Zhang ZH, Wei F, Vaziri ND, Cheng XL, Bai X, Lin RC, et al. Metabolomics insights into chronic kidney disease and modulatory effect of rhubarb against tubulointerstitial fibrosis. *Sci Rep*. 2015;5(1):14472. <https://doi.org/10.1038/srep14472>.
- Chen L, Cao G, Wang M, Feng YL, Chen DQ, Vaziri ND, et al. The matrix metalloproteinase-13 inhibitor poricoic acid zi ameliorates renal fibrosis by mitigating epithelial-mesenchymal transition. *Mol Nutr Food Res*. 2019;63:e1900132. <https://doi.org/10.1002/mnfr.201900132>.
- Liu X, Zhang B, Huang S, Wang F, Zheng L, Lu J, et al. Metabolomics analysis reveals the protection mechanism of Huangqi-Danshen decoction on adenine-induced chronic kidney disease in rats. *Front Pharmacol*. 2019;10:992. <https://doi.org/10.3389/fphar.2019.00992>.
- Ji C, Luo Y, Zou C, Huang L, Tian R, Lu Z. Effect of astragaloside IV on indoxyl sulfate-induced kidney injury in mice via attenuation of oxidative stress. *BMC Pharmacol Toxicol*. 2018;19(1):53. <https://doi.org/10.1186/s40360-018-0241-2>.
- Li Z, Zhu L, Zhang H, Yang J, Zhao J, Du D, et al. Protective effect of a polysaccharide from stem of *Codonopsis pilosula* against renal ischemia/reperfusion injury in rats. *Carbohydr Polym*. 2012;90(4):1739–43. <https://doi.org/10.1016/j.carbpol.2012.07.062>.
- Zheng X, Yu Y, Zhou J. Effects of chemical separation components and their compatibility on nephrotic syndrome in rats. *Chin J New Drugs Clin Pharmacol*. 2016;27(4):467–74.
- Lee D, Lee S, Shim SH, Lee HJ, Choi Y, Jang TS, et al. Protective effect of lanostane triterpenoids from the sclerotia of *Poria cocos* wolf against cisplatin-induced apoptosis in LLC-PK1 cells. *Bioorg Med Chem Lett*. 2017;27(13):2881–5. <https://doi.org/10.1016/j.bmcl.2017.04.084>.
- Qiao Y, Xu L, Tao X, Yin L, Qi Y, Xu Y, et al. Protective effects of dioscin against fructose-induced renal damage via adjusting Sirt3-mediated oxidative stress, fibrosis, lipid metabolism and inflammation. *Toxicol Lett*. 2018;284:37–45. <https://doi.org/10.1016/j.toxlet.2017.11.031>.
- Su J, Wei Y, Liu M, Liu T, Li J, Ji Y, et al. Anti-hyperuricemic and nephroprotective effects of *Rhizoma Dioscoreae septemlobae* extracts and its main component dioscin via regulation of mOAT1, mURAT1 and mOCT2 in hypertensive mice. *Arch Pharm Res*. 2014;37(10):1336–44. <https://doi.org/10.1007/s12272-014-0413-6>.

14. Lin EY, Bayarsengee U, Wang CC, Chiang YH, Cheng CW. The natural compound 2,3,5,4'-tetrahydroxystilbene-2-O-beta-D-glucoside protects against adriamycin-induced nephropathy through activating the Nrf2-Keap1 antioxidant pathway. *Environ Toxicol.* 2018;33(1):72–82. <https://doi.org/10.1002/tox.22496>.
15. Zhang J, Xu W, Wang P, Huang J, Bai J, Huang Z, et al. Chemical analysis and multi-component determination in Chinese medicine preparation Bupi Yishen formula using ultra-high performance liquid chromatography with linear ion trap-Orbitrap mass spectrometry and triple-quadrupole tandem mass spectrometry. *Front Pharmacol.* 2018;9:568. <https://doi.org/10.3389/fphar.2018.00568>.
16. Mao W, Zhang L, Zou C, Li C, Wu Y, Su G, et al. Rationale and design of the helping ease renal failure with Bupi Yishen compared with the angiotensin II antagonist losartan (HERBAAL) trial: a randomized controlled trial in non-diabetes stage 4 chronic kidney disease. *BMC Complement Altern Med.* 2015;15(1):316. <https://doi.org/10.1186/s12906-015-0830-1>.
17. Mao W, Yang N, Zhang L, Li C, Wu Y, Ouyang W, et al. Bupi Yishen formula versus losartan for non-diabetic stage 4 chronic kidney disease: a randomized controlled trial. *Front Pharmacol.* 2021;11:627185. <https://doi.org/10.3389/fphar.2020.627185>.
18. Johnson CH, Ivanisevic J, Siuzdak G. Metabolomics: beyond biomarkers and towards mechanisms. *Nat Rev Mol Cell Biol.* 2016;17(7):451–9. <https://doi.org/10.1038/nrm.2016.25>.
19. Miao X, Xiao B, Shui S, Yang J, Huang R, Dong J. Metabolomics analysis of serum reveals the effect of Danggui Buxue Tang on fatigued mice induced by exhausting physical exercise. *J Pharm Biomed Anal.* 2018;151:301–9. <https://doi.org/10.1016/j.jpba.2018.01.028>.
20. Xu P, Li S, Tian R, Han L, Mao W, Li L, et al. Metabonomic analysis of the therapeutic effects of Chinese medicine Sanqi Oral solution on rats with exhaustive exercise. *Front Pharmacol.* 2019;10:704. <https://doi.org/10.3389/fphar.2019.00704>.
21. Griffin KA, Picken M, Bidani AK. Method of renal mass reduction is a critical modulator of subsequent hypertension and glomerular injury. *J Am Soc Nephrol.* 1994;4(12):2023–31.
22. Spiers DE, Candas V. Relationship of skin surface area to body mass in the immature rat: a reexamination. *J Appl Physiol Respir Environ Exerc Physiol.* 1984;56(1):240–3. <https://doi.org/10.1152/jappl.1984.56.1.240>.
23. Liu X, Huang S, Wang F, Zheng L, Lu J, Chen J, et al. Huangqi-Danshen decoction ameliorates adenine-induced chronic kidney disease by modulating mitochondrial dynamics. *Evid Based Complement Alternat Med.* 2019;2019:9574045.
24. Li CY, Song HT, Wang XX, Wan YY, Ding XS, Liu SJ, et al. Urinary metabolomics reveals the therapeutic effect of Huangqi injections in cisplatin-induced nephrotoxic rats. *Sci Rep.* 2017;7(1):3619. <https://doi.org/10.1038/s41598-017-03249-z>.
25. Zhang M, Liu Y, Liu M, Liu B, Li N, Dong X, et al. UHPLC-QTOF/MS-based metabolomics investigation for the protective mechanism of Danshen in Alzheimer's disease cell model induced by Abeta1-42. *Metabolomics.* 2019;15(2):13. <https://doi.org/10.1007/s11306-019-1473-x>.
26. Zhang J, Wu C, Gao L, Du G, Qin X. Astragaloside IV derived from *Astragalus membranaceus*: a research review on the pharmacological effects. *Adv Pharmacol.* 2020;87:89–112. <https://doi.org/10.1016/bs.apha.2019.08.002>.
27. Zhang HF, Wang JH, Wang YL, Gao C, Gu YT, Huang J, et al. Salviaolic acid protects the kidney against oxidative stress by activating the Akt/GSK-3beta/Nrf2 signaling pathway and inhibiting the NF-kappaB signaling pathway in S/6 Nephrectomized rats. *Oxidative Med Cell Longev.* 2019;2019:2853534.
28. Quan W, Liu HX, Zhang W, Lou WJ, Gong YZ, Yuan C, et al. Cardioprotective effect of rosmarinic acid against myocardial ischaemia/reperfusion injury via suppression of the NF-kappaB inflammatory signalling pathway and ROS production in mice. *Pharm Biol.* 2021;59(1):222–31. <https://doi.org/10.1080/13880209.2021.1878236>.
29. Feng YL, Cao G, Chen DQ, Vaziri ND, Chen L, Zhang J, et al. Microbiome-metabolomics reveals gut microbiota associated with glycine-conjugated metabolites and polyamine metabolism in chronic kidney disease. *Cell Mol Life Sci.* 2019;76(24):4961–78. <https://doi.org/10.1007/s00018-019-03155-9>.
30. Wang A, Xiao Z, Zhou L, Zhang J, Li X, He Q. The protective effect of atractylenolide I on systemic inflammation in the mouse model of sepsis created by cecal ligation and puncture. *Pharm Biol.* 2016;54(1):146–50. <https://doi.org/10.3109/13880209.2015.1024330>.
31. Alkhalaf LM, Ryan KS. Biosynthetic manipulation of tryptophan in bacteria: pathways and mechanisms. *Chem Biol.* 2015;22(3):317–28. <https://doi.org/10.1016/j.chembiol.2015.02.005>.
32. Zelante T, Iannitti RG, Cunha C, De Luca A, Giovannini G, Pieraccini G, et al. Tryptophan catabolites from microbiota engage aryl hydrocarbon receptor and balance mucosal reactivity via interleukin-22. *Immunity.* 2013;39(2):372–85. <https://doi.org/10.1016/j.immuni.2013.08.003>.
33. Alexeev EE, Lanis JM, Kao DJ, Campbell EL, Kelly CJ, Battista KD, et al. Microbiota-derived indole metabolites promote human and murine intestinal homeostasis through regulation of Interleukin-10 receptor. *Am J Pathol.* 2018;188(5):1183–94. <https://doi.org/10.1016/j.ajpath.2018.01.011>.
34. Hubbard TD, Murray IA, Perdew GH. Indole and tryptophan metabolism: endogenous and dietary routes to an receptor activation. *Drug Metab Dispos.* 2015;43(10):1522–35. <https://doi.org/10.1124/dmd.115.064246>.
35. Clarke G, McKernan DP, Gaszner G, Quigley EM, Cryan JF, Dinan TG. A distinct profile of tryptophan metabolism along the kynurenine pathway downstream of toll-like receptor activation in irritable bowel syndrome. *Front Pharmacol.* 2012;3:90.
36. Cervenka I, Agudelo LZ, Ruas JL. Kynurenines: Tryptophan's metabolites in exercise, inflammation, and mental health. *Science.* 2017;357(6349):eaaf9794. <https://doi.org/10.1126/science.aaf9794>.
37. Kennedy PJ, Cryan JF, Dinan TG, Clarke G. Kynurenine pathway metabolism and the microbiota-gut-brain axis. *Neuropharmacology.* 2017;112(Pt B):399–412.
38. Yano JM, Yu K, Donaldson GP, Shastri GG, Ann P, Ma L, et al. Indigenous bacteria from the gut microbiota regulate host serotonin biosynthesis. *Cell.* 2015;161(2):264–76. <https://doi.org/10.1016/j.cell.2015.02.047>.
39. Dou L, Poitevin S, Sallée M, Addi T, Gondouin B, McKay N, et al. Aryl hydrocarbon receptor is activated in patients and mice with chronic kidney disease. *Kidney Int.* 2018;93(4):986–99. <https://doi.org/10.1016/j.kint.2017.11.010>.
40. Dou L, Sallée M, Cerini C, Poitevin S, Gondouin B, Jourde-Chiche N, et al. The cardiovascular effect of the uremic solute indole-3 acetic acid. *J Am Soc Nephrol.* 2015;26(4):876–87. <https://doi.org/10.1681/ASN.2013.12.1283>.
41. Clària J, Moreau R, Fenaille F, Amorós A, Junot C, Gronbaek H, et al. Orchestration of tryptophan-kynurenine pathway, acute decompensation, and acute-on-chronic liver failure in cirrhosis. *Hepatology.* 2019;69(4):1686–701. <https://doi.org/10.1002/hep.30363>.
42. Chen Y, Zelnick LR, Wang K, Hoofnagle AN, Becker JO, Hsu C-Y, et al. Kidney clearance of secretory solutes is associated with progression of CKD: the CRIC study. *J Am Soc Nephrol.* 2020;31(4):817–27. <https://doi.org/10.1681/ASN.2019080811>.
43. Pedersen ER, Tuset N, Eussen S, Ueland PM, Strand E, Svengen GFT, et al. Associations of plasma kynurenines with risk of acute myocardial infarction in patients with stable angina pectoris. *Arterioscler Thromb Vasc Biol.* 2015;35(2):455–62. <https://doi.org/10.1161/ATVBAHA.114.304674>.
44. Pawlak K, Domaniewski T, Mysliwiec M, Pawlak D. The kynurenines are associated with oxidative stress, inflammation and the prevalence of cardiovascular disease in patients with end-stage renal disease. *Atherosclerosis.* 2009;204(1):309–14. <https://doi.org/10.1016/j.atherosclerosis.2008.08.014>.
45. Karu N, McKercher C, Nichols DS, Davies N, Shellie RA, Hilder EF, et al. Tryptophan metabolism, its relation to inflammation and stress markers and association with psychological and cognitive functioning: Tasmanian chronic kidney disease pilot study. *BMC Nephrol.* 2016;17(1):171. <https://doi.org/10.1186/s12882-016-0387-3>.
46. Aronov PA, Luo FJ, Plummer NS, Quan Z, Holmes S, Hostetter TH, et al. Colonic contribution to uremic solutes. *J Am Soc Nephrol.* 2011;22(9):1769–76. <https://doi.org/10.1681/ASN.2010121220>.
47. Ujhelyi L, Balla G, Jeney V, Varga Z, Nagy E, Vercellotti G, et al. Hemodialysis reduces inhibitory effect of plasma ultrafiltrate on LDL oxidation and subsequent endothelial reactions. *Kidney Int.* 2006;69(1):144–51. <https://doi.org/10.1038/sj.ki.5000007>.
48. Jourde-Chiche N, Dou L, Calaf FSR, Robert CC, Charpiot LC-JP, Argiles A, et al. Levels of circulating endothelial progenitor cells are related to uremic toxins and vascular injury in hemodialysis patients. *J Thromb Haemost.* 2009;7(9):1576–84. <https://doi.org/10.1111/j.1538-7836.2009.03540.x>.
49. Wirthgen E, Otten W, Tuchscherer M, Tuchscherer A, Domanska G, Brenmoehl J, et al. Effects of 1-Methyltryptophan on immune responses and the kynurenine pathway after lipopolysaccharide challenge in pigs. *Int J Mol Sci.* 2018;19(10):3009. <https://doi.org/10.3390/ijms19103009>.

50. Małaczewska J, Siwicki AK, Wójcik RM, Turski WA, Kaczorek E. The effect of kynurenic acid on the synthesis of selected cytokines by murine splenocytes - in vitro and ex vivo studies. *Cent Eur J Immunol*. 2016;41(1):39–46. <https://doi.org/10.5114/ceji.2016.58815>.
51. Nicholl DDM, Hanly PJ, Poulin MJ, Handley GB, Hemmelgarn BR, Sola DY, et al. Evaluation of continuous positive airway pressure therapy on renin-angiotensin system activity in obstructive sleep apnea. *Am J Respir Crit Care Med*. 2014;190(5):572–80. <https://doi.org/10.1164/rccm.201403-0526OC>.
52. Ohashi N, Ishigaki S, Isobe S. The pivotal role of melatonin in ameliorating chronic kidney disease by suppression of the renin-angiotensin system in the kidney. *Hypertens Res*. 2019;42(6):761–8. <https://doi.org/10.1038/s41440-018-0186-2>.
53. Li N, Wang Z, Gao F, Lei Y, Li Z. Melatonin ameliorates renal fibroblast-myofibroblast transdifferentiation and renal fibrosis through miR-21-5p regulation. *J Cell Mol Med*. 2020;24(10):5615–28. <https://doi.org/10.1111/jcmm.15221>.
54. Ebaid H, Bashandy SAE, Abdel-Mageed AM, Al-Tamimi J, Hassan I, Alhazza IM. Folic acid and melatonin mitigate diabetic nephropathy in rats via inhibition of oxidative stress. *Nutr Metab (Lond)*. 2020;17(1):6. <https://doi.org/10.1186/s12986-019-0419-7>.
55. Mo Y, Lu Z, Wang L, Ji C, Zou C, Liu X. The aryl hydrocarbon receptor in chronic kidney disease: friend or foe? *Front Cell Dev Biol*. 2020;8:589752. <https://doi.org/10.3389/fcell.2020.589752>.
56. Kimura A, Naka T, Nohara K, Fujii-Kuriyama Y, Kishimoto T. Aryl hydrocarbon receptor regulates Stat1 activation and participates in the development of Th17 cells. *Proc Natl Acad Sci U S A*. 2008;105(28):9721–6. <https://doi.org/10.1073/pnas.0804231105>.
57. Singh R, Chandrashekarappa S, Bodduluri SR, Baby BV, Hegde B, Kotla NG, et al. Enhancement of the gut barrier integrity by a microbial metabolite through the Nrf2 pathway. *Nat Commun*. 2019;10(1):89. <https://doi.org/10.1038/s41467-018-07859-7>.
58. Wang G, Zhang L, Zhao X, Gao S, Qu L, Yu H, et al. The aryl hydrocarbon receptor mediates tobacco-induced PD-L1 expression and is associated with response to immunotherapy. *Nat Commun*. 2019;10(1):1125. <https://doi.org/10.1038/s41467-019-08887-7>.
59. Jaeger C, Tischkau SA. Role of aryl hydrocarbon receptor in circadian clock disruption and metabolic dysfunction. *Environ Health Insights*. 2016;10:133–41. <https://doi.org/10.4137/EHI.S38343>.
60. Bao A, Yang H, Ji J, Chen Y, Bao W, Li F, et al. Involvements of p38 MAPK and oxidative stress in the ozone-induced enhancement of AHR and pulmonary inflammation in an allergic asthma model. *Respir Res*. 2017;18(1):216. <https://doi.org/10.1186/s12931-017-0697-4>.
61. Sayed N, Khurana A, Godugu C. Pharmaceutical perspective on the translational hurdles of phytoconstituents and strategies to overcome. *J Drug Deliv Sci Technol*. 2019;53:101201. <https://doi.org/10.1016/j.jddst.2019.101201>.
62. Lin T-L, Lu C-C, Lai W-F, Wu T-S, Lu J-J, Chen Y-M, et al. Role of gut microbiota in identification of novel TCM-derived active metabolites. *Protein Cell*. 2021;12(5):394–410. <https://doi.org/10.1007/s13238-020-00784-w>.

Publisher's Note

Springer Nature remains neutral with regard to jurisdictional claims in published maps and institutional affiliations.

Ready to submit your research? Choose BMC and benefit from:

- fast, convenient online submission
- thorough peer review by experienced researchers in your field
- rapid publication on acceptance
- support for research data, including large and complex data types
- gold Open Access which fosters wider collaboration and increased citations
- maximum visibility for your research: over 100M website views per year

At BMC, research is always in progress.

Learn more biomedcentral.com/submissions

